

# Preparation of Cross-Linked Polystyrene Hollow Nanospheres via Surface-Initiated Atom Transfer Radical Polymerizations

G. D. Fu, Zhenhua Shang, Liang Hong, E. T. Kang,\* and K. G. Neoh

Department of Chemical & Biomolecular Engineering,  
National University of Singapore, Kent Ridge,  
Singapore 119260

Received April 30, 2005

Revised Manuscript Received July 3, 2005

## Introduction

Hollow micro- and nanospheres are potentially useful as encapsulation agents for controlled release of drugs,<sup>1–3</sup> catalyst,<sup>4</sup> paints,<sup>4</sup> and enzymes,<sup>3</sup> as transducers for electronics,<sup>5</sup> and as absorption materials for sound.<sup>5</sup> To meet the requirements for encapsulation, various hollow spheres of carbon,<sup>6,7</sup> polymers,<sup>8,9</sup> metal,<sup>10,11</sup> and inorganic materials<sup>1,12–14</sup> have been prepared using polymeric or inorganic spherical particles as the templates.

Polymeric hollow spheres have been prepared by removal of the hydrocarbon solvent encapsulated in the core of polymer particles from emulsion polymerization,<sup>15–17</sup> by self-assembly of rod-coil block copolymers,<sup>18</sup> from micelle formation of block copolymers,<sup>19–21</sup> and via the lost-wax method.<sup>22</sup> Recent development in surface-initiated controlled/living polymerizations provides a means for preparing inorganic/organic core-shell hybrids with well-defined shell structure and thickness.<sup>23–27</sup> Nearly monodispersed hollow spheres of 150 nm to 4  $\mu$ m in size with controllable shell thickness were prepared from removal of the core templates of the core-shell composites.<sup>28–31</sup> Accordingly, the preparation of cross-linked and solvent-resistant polymer hollow nanospheres should be of interest.

It is well known that polystyrene (PS) and poly(methyl methacrylate) (PMMA) have significantly different photochemical properties.<sup>32</sup> Under ultraviolet (UV) irradiation, PMMA (as a positive photoresist) will degrade via chain scission,<sup>33–35</sup> while PS (as a negative photoresist) will undergo cross-linking under proper conditions.<sup>36</sup> Well-defined nanoscopic templates have been prepared by UV treatment of PS-PMMA block copolymers.<sup>37</sup> Even though cross-linked hollow nanospheres have been prepared by chemical cross-linking<sup>19,20,31</sup> and UV-induced cross-linking,<sup>21</sup> the preparation of hollow nanospheres via surface-initiated living radical polymerization and UV-induced cross-linking remains attractive because of the well-controlled core void and well-defined shell thickness achievable, in addition to the simplicity of the UV-induced cross-linking process.

In the present work, hollow nanospheres with cross-linked PS shell were prepared, as illustrated in Scheme 1. Initially, the atom transfer radical polymerization (ATRP) initiators were immobilized onto the surface of SiO<sub>2</sub> nanoparticles of about 25 nm in diameter. Silica nanoparticles with surface-grafted block copolymer of styrene and methyl methacrylate (SiO<sub>2</sub>-*g*-PS-*b*-PMMA) were prepared via surface-initiated ATRP of styrene and subsequently ATRP of methyl methacrylate. The nano-

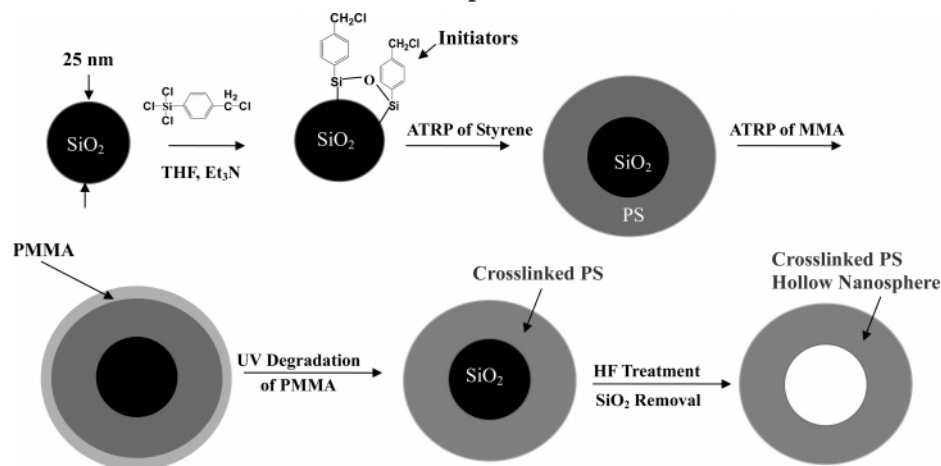
composites were cast into films of about 3  $\mu$ m in thickness. Exposure to UV ( $\lambda$  = 254 nm) resulted in cross-linking of the PS shell and decomposition of the PMMA outer layer. The sacrificial PMMA outer shell prevented interparticle cross-linking and agglomeration of the PS nanospheres. After removal of the SiO<sub>2</sub> core by HF etching, well-defined hollow nanospheres with cross-linked PS shell of about 20–60 nm in thickness and void cores of about 20–30 nm in diameter were obtained. The core-shell structures of SiO<sub>2</sub>-*g*-PS and SiO<sub>2</sub>-*g*-PS-*b*-PMMA, and of the cross-linked PS hollow nanospheres, were characterized by X-ray photoelectron spectroscopy (XPS), transmission electron microscopy (TEM), and energy-dispersive X-ray (EDX) analysis. The cleaved PS and PS-*b*-PMMA from the silica surfaces were characterized by gel-permeation chromatography (GPC) and <sup>1</sup>H NMR spectroscopy.

## Results and Discussion

Initially, the ATRP initiator, trichloro(4-chloromethylphenyl)silane, was immobilized on the silica particles of about 25 nm in diameter through the reaction of the chlorosilyl group with the silanol group. A transmission electron microscopy (TEM) image of the initiator-immobilized silica nanoparticles is shown in Figure 1a. The field emission scanning electron microscopy (FESEM) image of the sample (inset of Figure 1a) shows that the surface-modified nanoparticles remain unagglomerated. Figure 2a shows the X-ray photoelectron spectroscopy (XPS) wide scan spectrum of the initiator-immobilized silica nanoparticles. The peak component at the binding energy (BE) of about 200 eV, attributable to the covalent Cl 2p species, indicates that the benzyl chloride initiators have been successfully immobilized on the silica surface. The relative amount of benzyl chloride on the surface of silica particles was revealed by energy-dispersive X-ray (EDX) analysis (Figure 3a). The signals at 2.65 and 0.25 keV are attributable to chlorine and carbon, respectively. The chlorine concentration of about 1.28 wt % is in reasonable agreement with that of 1.44 wt % obtained from elemental analysis. The corresponding surface benzyl chloride initiator content of about 2.4 initiators/nm<sup>2</sup> (based on the Cl concentration of 1.44 wt %) is comparable to the reported silane initiator density of 2.6 initiators/nm<sup>2</sup> for the silica particle surface.<sup>23</sup>

The silica-graft-polystyrene hybrid (SiO<sub>2</sub>-*g*-PS) was prepared via surface-initiated ATRP of styrene from the initiator-immobilized silica nanoparticles, using CuCl/N,N,N',N'',N'''-pentamethyldiethylenetriamine (PMDETA) as the catalyst system. Figure 1b shows the TEM micrograph of the SiO<sub>2</sub>-*g*-PS2 nanoparticles described in Table 1. A basically core-shell structure (dark-colored core for SiO<sub>2</sub> and light-colored shell for PS) was obtained. The composition of the core-shell structure was also confirmed by XPS analysis. The appearance of a strong C 1s peak component and the disappearance of Si 2p species in the XPS wide scan spectrum of Figure 2b are consistent with the presence of a SiO<sub>2</sub>-*g*-PS core-shell structure, with a shell thickness greater than the sampling depth of the XPS technique (about 7.5 nm in an organic matrix<sup>38</sup>). The thickness of the PS shell can be adjusted by changing the polymerization time.<sup>11,23</sup> The shell thicknesses of the SiO<sub>2</sub>-*g*-PS nanospheres corresponding to different reaction time are summarized

\* To whom correspondence should be addressed: Tel 65-68742189; Fax 65-67791936; e-mail cheket@nus.edu.sg.

**Scheme 1. Schematic Illustration of the Process for the Preparation of Cross-Linked Polystyrene (PS) Hollow Nanospheres<sup>a</sup>**

<sup>a</sup> THF = tetrahydrofuran, ATRP = atom transfer radical polymerization, MMA = methyl methacrylate, PMMA = poly(methyl methacrylate), HF = hydrofluoric acid, and Et<sub>3</sub>N = triethylamine.

in Table 1. As the polymerization time is increased from 1.5 to 6.0 h, the thickness of the PS shell increases correspondingly from 21 to 46 nm. The gel permeation chromatograph (GPC) results of PS cleaved from the SiO<sub>2</sub>-*g*-PS nanoparticles indicate that, with the increase in polymerization time from 1.5 to 6 h, the number-average molecular weight ( $M_n$ ) increases from  $1.4 \times 10^4$  to  $5.4 \times 10^4$  g/mol, while the polydispersity index remains at around 1.2.

Surface-initiated atom transfer block copolymerization of MMA from the SiO<sub>2</sub>-*g*-PS nanospheres, using CuBr/PMDETA as the catalyst system, gave rise to the SiO<sub>2</sub>-*g*-PS-*b*-PMMA nanospheres. The halide exchange reaction can give rise to a fast initiation and improve the control of ATRP.<sup>39</sup> The TEM image of the resulting nanospheres reveals an increase in particle size and shell thickness of the SiO<sub>2</sub>-*g*-PS-*b*-PMMA nanospheres, in comparison with the starting SiO<sub>2</sub>-*g*-PS nanospheres, consistent with the addition of an additional PMMA shell. Furthermore, the appearance of an O 1s peak component at the BE of about 532 eV (Figure 2c), and a marked increase in C content and decrease in Si content in the EDX spectrum (Figure 3b), are consistent with the presence of a PMMA graft layer on the Si-*g*-PS nanospheres. The successful preparation of SiO<sub>2</sub>-*g*-PS-*b*-PMMA nanospheres was also confirmed by <sup>1</sup>H NMR spectroscopy and GPC results of the PS-*b*-PMMA block copolymers cleaved from the silica surface (Table 1). In comparison with the <sup>1</sup>H NMR spectrum of the PS chains cleaved from the silica surface, the appearance of chemical shifts at 0.9–0.11 and 3.6 ppm (attributable to C–CH<sub>3</sub> and O–CH<sub>3</sub> groups, respectively, of the PMMA block) in the <sup>1</sup>H NMR spectrum of the cleaved PS-*b*-PMMA copolymers confirms the successful preparation of the SiO<sub>2</sub>-*g*-PS-*b*-PMMA nanospheres.

UV exposure of the SiO<sub>2</sub>-*g*-PS-*b*-PMMA nanospheres decomposes the PMMA outer shell and cross-linked the PS shell. Subsequent HF etching removes the SiO<sub>2</sub> core. The TEM image in Figure 1c (from SiO<sub>2</sub>-*g*-PS-*b*-PMMA3 in Table 1) clearly reveals the hollow structure of the nanospheres with a shell thickness of about 40 nm. The presence of a cross-linked shell has given rise to a well-preserved nanospherical structure in THF (a good solvent for PS). Comparing to their precursor nanospheres (SiO<sub>2</sub>-*g*-PS-*b*-PMMA3 in Table 1), the shell thickness of the hollow spheres has decreased from

about 51 nm to about 41 nm after the UV treatment. The UV-treated film of SiO<sub>2</sub>-*g*-PS nanoparticles without the PMMA outer shell cannot be redispersed into THF, indicating that the SiO<sub>2</sub>-*g*-PS nanoparticles have undergone interparticle cross-linking in the absence of the sacrificial PMMA outer shell. Thus, the decomposition of a thin PMMA outer shell has effectively prevented cross-linking among the PS nanoparticles. The almost complete disappearance of the Si and oxygen signals and the predominance of carbon signal in the EDX results of Figure 3c are consistent with the formation of PS hollow nanospheres. The PS hollow nanospheres of different shell thicknesses prepared from different SiO<sub>2</sub>-*g*-PS-*b*-PMMA particles are summarized in Table 1. With the  $M_n$  of PS increases from  $1.4 \times 10^4$  to  $5.4 \times 10^4$  g/mol, the shell thickness of the hollow nanospheres increases correspondingly from 18 to 41 nm.

## Conclusions

Cross-linked PS hollow nanospheres can be prepared by UV treatment of the SiO<sub>2</sub>-*g*-PS-*b*-PMMA core-shell hybrids and HF etching of the SiO<sub>2</sub> cores. The surface-initiated ATRP's allow the preparation of well-defined PS and PS-*b*-PMMA shell structures. The cross-linked PS hollow nanospheres remain unagglomerated and stable in organic solvents, such as THF. The shell thickness of SiO<sub>2</sub>-*g*-PS-*b*-PMMA can be readily tuned by controlling the PMMA and PS chain lengths during the ATRP process. The present solvent-resistant PS hollow nanospheres are potentially useful in applications such as controlled release and enzyme immobilization and as nanoreactors.

## Experimental Section

**Initiator Immobilization on Silica Particles.** Dried SiO<sub>2</sub> particles (2.0 g) of sizes in the range 20–30 nm, 3.0 g (9.5 mmol) of trichloro(4-chloromethylphenyl)silane (97%), and 20 mL of absolutely dried THF were introduced into a two-necked flask. Triethylamine (1.2 mL, 8.6 mmol) in THF (5.0 mL) was added dropwise, with stirring, under an argon environment. The reaction mixture was left to stand for 8 h and then exposed to air for another 18 h. After five cycles of ethanol and THF rinsing, and separation by centrifugation, about 1.8 g of white initiator-immobilized SiO<sub>2</sub> particles was obtained. The chloride concentration was about 1.44 wt %, as determined from elemental analysis. This chlorine concentration corresponded to about 2.4 benzyl chloride initiators per nm<sup>2</sup> of the particle surface.

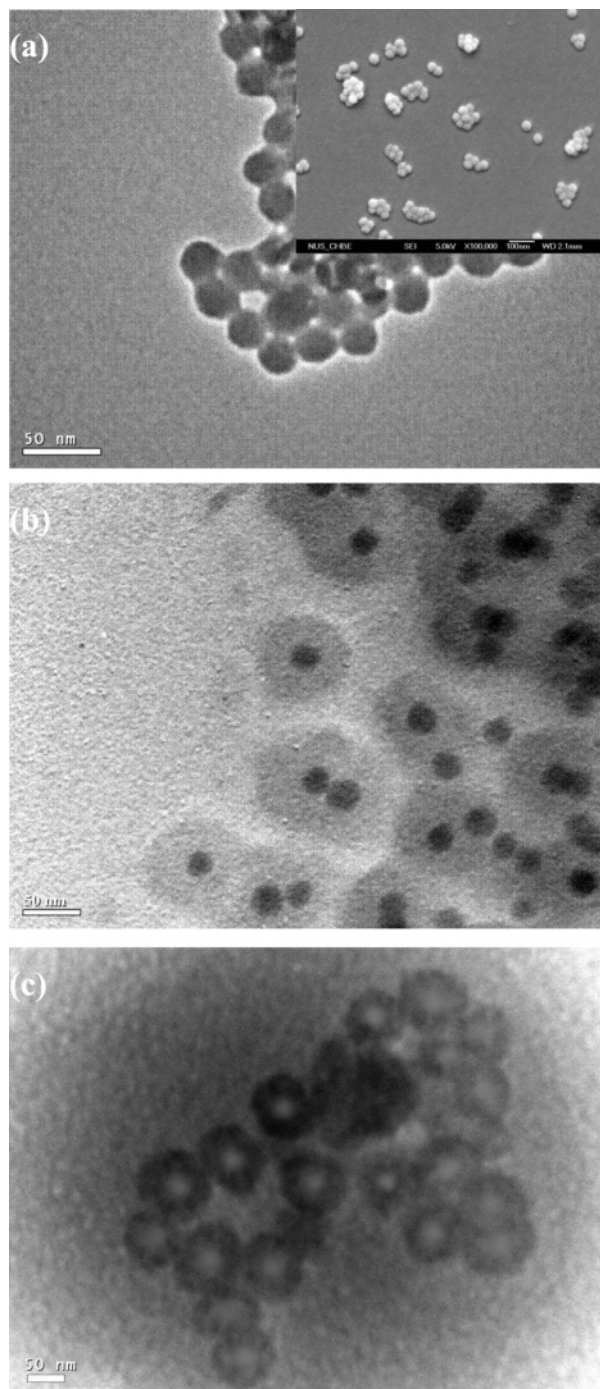


**Figure 1.** Transmission electron microscopy (TEM) micrographs (a) of the initiator-immobilized silica nanoparticles, (b) silica-graft-polystyrene nanospheres ( $\text{SiO}_2\text{-g-PS2}$  in Table 1; surface-initiated atom transfer radical polymerization (ATRP) conditions: [styrene]:[initiator]:[CuCl]:[PMDETA] = 800:1:1:1; polymerization time = 3 h), and (c) cross-linked polystyrene (PS) hollow nanospheres obtained via UV treatment and HF etching of the silica-graft-polystyrene-block-poly(methyl methacrylate) nanospheres ( $\text{SiO}_2\text{-g-PS-}b\text{-PMMA3}$  in Table 1, prepared from the corresponding  $\text{SiO}_2\text{-g-PS}$  nanospheres, using the active PS chain ends as the macroinitiators under otherwise the same conditions as those used for the initial surface-initiated ATRP of styrene). The field emission scanning electron microscopy (FESEM) image in the inset of (a) shows that the initiator-immobilized silica nanoparticles remain segregated.

**Surface-Initiated ATRP.** About 0.1 g of the initiator-immobilized silica particles, 4 mL (0.035 mol) of styrene (99%), 4 mL of dry DMF, and 4 mg (0.04 mmol) of CuCl (99%) were introduced into a dry Pyrex test tube. After purging with argon

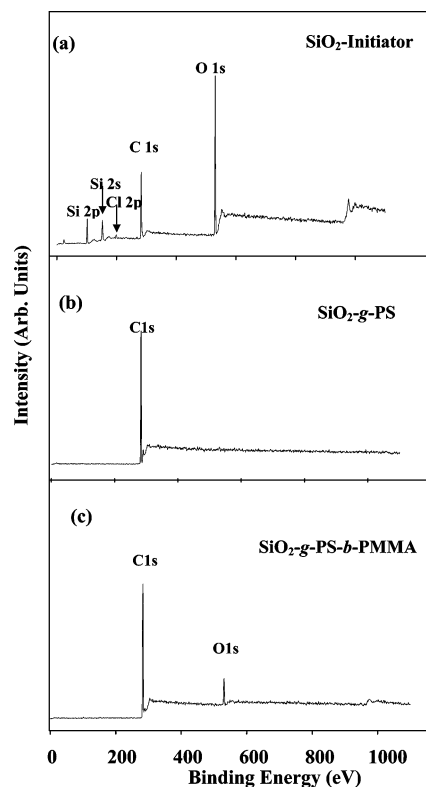


**Figure 2.** X-ray photoelectron spectroscopy (XPS) wide-scan spectra of the (a) initiator-immobilized silica particles, (b) silica-graft-polystyrene nanospheres ( $\text{SiO}_2\text{-g-PS3}$  in Table 1; surface-initiated atom transfer radical polymerization (ATRP) conditions: [styrene]:[initiator]:[CuCl]:[PMDETA] = 800:1:1:1; polymerization time = 6 h), and (c) silica-graft-polystyrene-block-poly(methyl methacrylate) nanospheres ( $\text{SiO}_2\text{-g-PS-}b\text{-PMMA3}$  in Table 1, prepared from the corresponding  $\text{SiO}_2\text{-g-PS}$  nanospheres, using the active PS chain ends as the macroinitiators under otherwise the same conditions as those used for the initial surface-initiated ATRP of styrene).

for 20 min, about 10  $\mu\text{L}$  (0.04 mmol) of  $N,N,N',N'',N'''$ -pentamethyldiethylenetriamine (PMDETA, 99%) was added, and the tube was sealed with a rubber stop. Thus, the molar ratio of [styrene]:[initiator]:[CuCl]:[PMDETA] was 800:1:1:1. Surface-initiated ATRP was carried out under continuous stirring at 110  $^{\circ}\text{C}$ . The reaction was allowed to proceed for 1.5, 3.0, and 6.0 h. At the end of each reaction, the reaction mixture was diluted with 30 mL of THF and precipitated in 200 mL of methanol. The product was redispersed in 40 mL of THF and centrifuged to remove the PS homopolymer. The process was repeated twice. The surface-initiated atom transfer block copolymerization of MMA was carried out using the same procedure as that used for styrene polymerization, except the  $\text{SiO}_2\text{-g-PS}$  nanoparticles (0.2 g) was used as the macroinitiators instead. The ATRP was allowed to proceed for 2 h to give rise to the  $\text{SiO}_2\text{-g-PS-}b\text{-PMMA}$  nanospheres. Cleavage of the PS and PS- $b$ -PMMA graft chains from the respective  $\text{SiO}_2\text{-g-PS}$  and  $\text{SiO}_2\text{-g-PS-}b\text{-PMMA}$  nanoparticle surfaces was achieved by dispersing 0.2 g of the respective nanoparticles in 2 mL of 10% HF for 2 h. About 10 mL of THF was then added to dissolve the PS homopolymer or the PS- $b$ -PMMA copolymer. The polymer or copolymer was recovered by precipitation in 50 mL of methanol.

**Formation of the Hollow Silica Nanospheres.** The  $\text{SiO}_2\text{-g-PS-}b\text{-PMMA}$  nanospheres dispersed in THF (0.02 g/mL) were deposited onto a clean Si(100) substrate surface. The film with a thickness of about 3  $\mu\text{m}$  was irradiated at a distance of about 5 cm for 15 min with an 800 W mercury UV lamp having a maximum emission at 254 nm. Then, the film was immersed into 10% HF at room temperature for 2 h to dissolve the  $\text{SiO}_2$  cores. The film was subsequently redispersed into THF, followed by washing and centrifugation with THF for another

Table 1. Molecular Weights and Shell Thickness of the Polystyrene Nanospheres

sample	polymerization time (h)	mol wt <sup>a</sup> (g/mol)	PDI <sup>a</sup>	particle size <sup>d</sup> (nm)	shell thickness <sup>d</sup> (nm)	shell thickness <sup>e</sup> (nm)
SiO <sub>2</sub> -g-PS1 <sup>b</sup>	1.5	$1.4 \times 10^4$	1.24	64	21	
SiO <sub>2</sub> -g-PS2 <sup>b</sup>	3.0	$3.1 \times 10^4$	1.28	100	37	
SiO <sub>2</sub> -g-PS3 <sup>b</sup>	6.0	$5.4 \times 10^4$	1.23	142	46	
SiO <sub>2</sub> -g-PS- <i>b</i> -PMMA1 <sup>c</sup>	2.0	$2.9 \times 10^4$	1.32	81	27	18
SiO <sub>2</sub> -g-PS- <i>b</i> -PMMA2 <sup>c</sup>	2.0	$4.8 \times 10^4$	1.34	123	44	24
SiO <sub>2</sub> -g-PS- <i>b</i> -PMMA3 <sup>c</sup>	2.0	$6.7 \times 10^4$	1.33	161	51	41

<sup>a</sup> Number-average molecular weight ( $M_n$ ) and polydispersity ( $PDI = M_w/M_n$ , where  $M_w$  is weight-average molecular weight) of the cleaved polystyrene (PS) and polystyrene-*block*-poly(methyl methacrylate) (PS-*b*-PMMA) chains from SiO<sub>2</sub> nanoparticles. <sup>b</sup> The molar ratio of [styrene]:[initiator]:[CuCl]:[PMDETA] = 800:1:1:1 for the surface-initiated atom transfer radical polymerization (ATRP) of styrene. The amount of initiators on the SiO<sub>2</sub> surface was determined from the element analysis results. PMDETA = *N,N,N',N'',N'''*-pentamethyldiethylenetriamine. <sup>c</sup> The block copolymer was prepared from the corresponding SiO<sub>2</sub>-g-PS nanospheres, using the active PS chain ends as the macroinitiators under otherwise the same conditions as those used for the initial surface-initiated ATRP of styrene. SiO<sub>2</sub>-g-PS = silica-*graft*-polystyrene and SiO<sub>2</sub>-g-PS-*b*-PMMA = silica-*graft*-polystyrene-*block*-poly(methyl methacrylate). <sup>d</sup> Average particle size and shell thickness of the nanospheres, determined from TEM images, before UV treatment. <sup>e</sup> Average shell thickness of the hollow nanospheres, determined from TEM images, after UV treatment and HF etching.

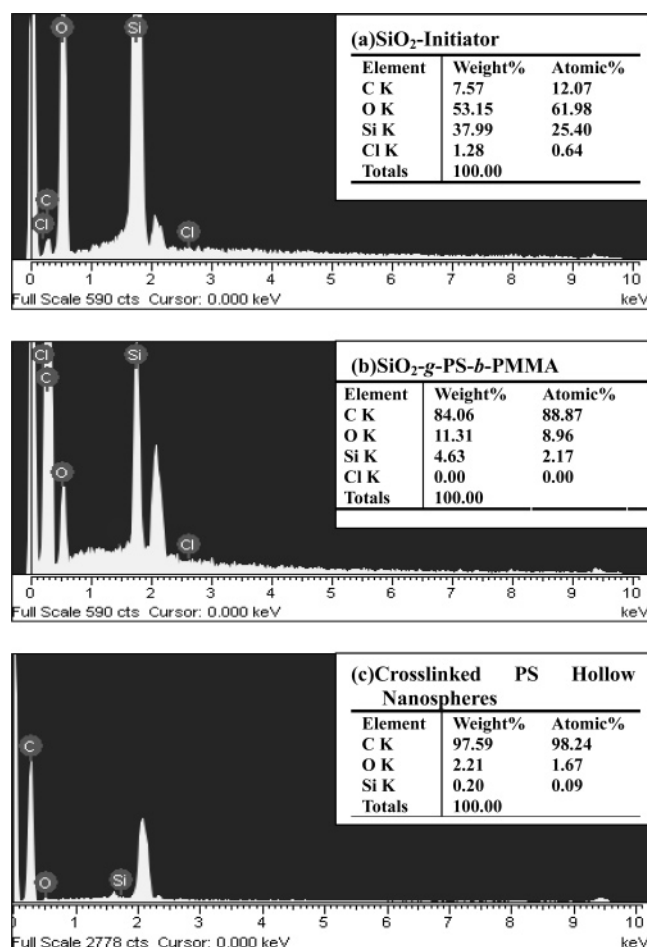


**Figure 3.** Energy-dispersive X-ray (EDX) analysis spectra of the (a) initiator-immobilized silica nanoparticles, (b) silica-*graft*-polystyrene-*block*-poly(methyl methacrylate) nanoparticles (SiO<sub>2</sub>-g-PS-*b*-PMMA3 in Table 1, prepared from the corresponding SiO<sub>2</sub>-g-PS nanospheres, using the active PS chain ends as the macroinitiators and surface-initiated ATRP conditions of [MMA]:[macroinitiator]:[CuCl]:[PMDETA] ~ 800:1:1:1 for 2 h), and (c) cross-linked polystyrene (PS) hollow nanospheres obtained from UV treatment and HF etching of the SiO<sub>2</sub>-g-PS-*b*-PMMA3 nanoparticles.

two times to obtain the cross-linked PS hollow nanospheres. About 0.06 g of unagglomerated nanospheres was obtained.

**Characterization.** Gel permeation chromatography (GPC) was performed on an HP 1100 HPLC, equipped with a HP 1047A refractive index detector and a PLgel MIXED-C 300 × 7.5 mm column (packed with 5 μm particles of different pore size). The column packing allowed the separation of polymers

over a wide molecular weight range of 200–3 000 000. THF was used as the eluent at a flow rate of 1 mL/min at 35 °C. Polystyrene standards were used as the references. XPS measurements were carried out on a Kratos AXIS HSi spectrometer (Kratos Analytical Ltd., Manchester, England) with a monochromatized Al Kα X-ray source (1486.6 eV photons). A JEOL 2010 TEM was used to characterize the morphology of the nanoparticles. Field emission scanning electron microscopy (FESEM) measurements were carried out on a JEOL JSM-6700 FESEM. Energy-dispersive X-ray (EDX) analysis spectra of the samples were obtained on a JEOL JSM5600LV scanning electron microscope. <sup>1</sup>H NMR spectra were measured on a Bruker ARX 300 MHz spectrometer, using CDCl<sub>3</sub> as the solvent. Elemental analyses were carried out on a Perkin-Elmer model 2400 elemental analyzer. The Cl content was determined by the Schöniger combustion method.<sup>40</sup>

## References and Notes

- Caruso, F.; Caruso, R. A.; Möhwald, H. *Science* **1998**, *282*, 1111–1114.
- Wilcox, D. L.; Berg, M.; Bernat, T.; Kellerman, D.; Cochran, J. K. *Hollow and Solid Spheres and Microspheres: Science and Technology Associated with Their Fabrication and Application*; Materials Research Society Proceedings: Pittsburgh, 1995; p 372.
- Gill, I.; Ballesteros, A. *J. Am. Chem. Soc.* **1998**, *120*, 8587–8598.
- Morris, C. A.; Anderson, M. L.; Stround, R. M.; Merzbacher, C. I.; Rolison, D. R. *Science* **1999**, *284*, 622–624.
- Cochran, J. K. *Curr. Opin. Solid State Mater. Sci.* **1998**, *3*, 474.
- Kawashashi, N.; Matijevic, E. *J. Colloid Interface Sci.* **1991**, *143*, 103–115.
- Chang, S.; Liu, L.; Asher, S. *J. Am. Chem. Soc.* **1994**, *116*, 6745–6747.
- Lee, J.; Sohn, K.; Hyeon, T. *J. Am. Chem. Soc.* **2001**, *123*, 5146–5147.
- Yoon, S. B.; Sohn, K.; Kim, J. Y.; Shin, C.-H.; Yu, J.-S.; Hyeon, T. *Adv. Mater.* **2002**, *14*, 19–21.
- Donath, E.; Sukhorucov, G. B.; Caruso, F.; Davis, S. A.; Möhwald, H. *Angew. Chem., Int. Ed.* **1998**, *37*, 2202–2204.
- Mandal, T. K.; Fleming, M. S.; Walt, D. R. *Chem. Mater.* **2000**, *12*, 3481–3487.
- Egan, G. L.; Yu, J. S.; Kim, C. H.; Lee, S. J.; Schak, R. E.; Mallouk, T. E. *Adv. Mater.* **2000**, *12*, 1040–1042.
- Graf, C.; Vossen, D. L. J.; Imhof, A.; Blaaderen, A. V. *Langmuir* **2003**, *19*, 6693–6700.
- Chen, Y.; Kang, E. T.; Neoh, K. G.; Greiner, A. *Adv. Funct. Mater.* **2005**, *15*, 113–117.
- Kowalski, A.; Vogel, M.; Blankenship, R. M. U.S. Patent No. 4,427,836, 1984.
- Blankenship, R. M.; Kowalski, A. U.S. Patent No. 4,594,363, 1986.
- Marinakos, C. J.; Bouck, K. J.; Bruce, C.; Stevens, A. C. *J. Macromolecules* **2000**, *33*, 1593–1597.
- Jenekhe, S. A.; Chen, X. L. *Science* **1999**, *283*, 372–375.

- (19) Ma, Q.; Remsen, E. E.; Kowalewski, T.; Wooley, K. L. *J. Am. Chem. Soc.* **2001**, *123*, 4627–4628.
- (20) Zhang, Q.; Remsen, E. E.; Wooley, K. L. *J. Am. Chem. Soc.* **2000**, *122*, 3642–3651.
- (21) Stewart, S.; Liu, G. *Chem. Mater.* **1999**, *11*, 1048–1054.
- (22) Jiang, P.; Bertone, J. F.; Colvin, V. L. *Science* **2001**, *291*, 453–457.
- (23) von Werne, T.; Patten, T. E. *J. Am. Chem. Soc.* **2001**, *123*, 7497–7505.
- (24) von Werne, T.; Patten, T. E. *J. Am. Chem. Soc.* **1999**, *121*, 7409–7410.
- (25) Wang, J. S.; Matyjaszewski, K. *J. Am. Chem. Soc.* **1995**, *117*, 5614–5615.
- (26) Hawker, C. J. *Acc. Chem. Res.* **1997**, *30*, 373–375.
- (27) Mori, H.; Seng, D. C.; Zhang, M.; Muller, A. H. *Langmuir* **2002**, *18*, 3382–3693.
- (28) Mandal, T. K.; Fleming, M. S.; Walt, D. R. *Chem. Mater.* **2000**, *12*, 3481–3487.
- (29) Xu, X. L.; Asher, S. A. *J. Am. Chem. Soc.* **2004**, *126*, 7940–7945.
- (30) Reiser, A. *Photoreactive Polymer-the Science and Technology of Resist*; Wiley: New York, 1989; p 18.
- (31) Kamata, K.; Lu, Y.; Xia, Y. *J. Am. Chem. Soc.* **2003**, *125*, 2384–2385.
- (32) Blomberg, S.; Ostbrg, S.; Harth, E.; Bosman, A. W.; Horn, B. V.; Hawker, C. J. *J. Polym. Sci., Part A: Polym. Chem.* **2002**, *40*, 1309–1320.
- (33) Kaczmarek, H.; Kaminska, A.; van Herk, A. *Eur. Polym. J.* **2000**, *36*, 767–776.
- (34) Caykara, T.; Guven, O. *Polym. Degrad. Stab.* **1999**, *65*, 225–234.
- (35) Forsythe, J. S.; Hill, D. J. T. *Prog. Polym. Sci.* **2000**, *25*, 101–136.
- (36) Ranby, B.; Rabek, J. F. *Photodegradation, Photo-Oxidation and Photostability of Polymers*; Wiley: New York, 1975; p 36.
- (37) Thurn-Albrecht, T.; Steiner, R.; Derouchey, J.; Staffor, C. M.; Huang, E.; Bal, M.; Tuominen, M.; Hawker, C. J.; Russell, T. P. *Adv. Mater.* **2000**, *12*, 787–781.
- (38) Tan, K. L.; Woon, L. L.; Wong, H. K.; Kang, E. T.; Neoh, K. G. *Macromolecules* **1993**, *26*, 2832–2836.
- (39) Matyjaszewski, K.; Shipp, D. A.; Wang, J. L.; Grimaud, T.; Patten, T. E. *Macromolecules* **1998**, *31*, 6836–6840.
- (40) Walthon, H. F. *Principles and Methods of Chemical Analysis*, 2nd ed.; Prentice Hall: Englewood Cliffs, NJ, 1964; p 24.

MA0509098